THE JOURNAL OF PHYSICAL CHEMISTRY B

ARTICLE

pubs.acs.org/JPCB

Biophysical Characterization of Complexes of DNA with Mixtures of the Neutral Lipids 1,2-Dioleoyl-*sn*-glycero-3-phosphoethanolamine-*N*-hexanoylamine or 1,2-Dioleoyl-*sn*-glycero-3-phosphoethanolamine-*N*-dodecanoylamine and 1,2-Dioleoyl-*sn*-glycero-3-phosphocholine in the Presence of Bivalent Metal Cations for DNA Transfection

Michela Pisani,*[,†] Giovanna Mobbili,[†] Immacolata F. Placentino,[†] Arianna Smorlesi,[‡] and Paolo Bruni[†]

[†]Chemistry Division of the ISAC Department, Polytechnic University of Marche, Via Brecce Bianche, 60131 Ancona, Italy

[‡]Department of Pathology and Innovative Therapies, Polytechnic University of Marche, Via Tronto 10/A, 60100 Ancona, Italy

ABSTRACT:

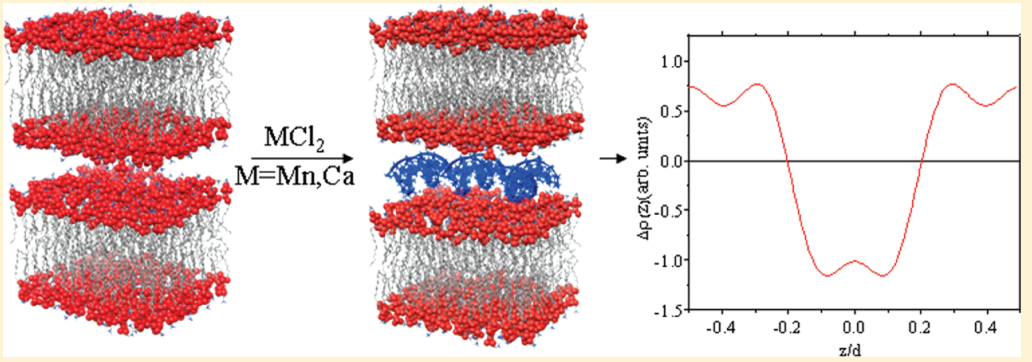

Neutral lipids have received up to now a little attention as genetic material carriers, despite some valuable features, such as the absence of toxicity and the high stability in serum of their complexes with DNA. We have prepared two quaternary complexes of DNA and mixtures of 1, 2-dioleoyl-*sn*-glycero-3-phosphoethanolamine-*N*-hexanoylamine (6PE) or 1,2-dioleoyl-*sn*-glycero-3-phosphoethanolamine-*N*-dodecanoylamine (12PE) with DOPC in aqueous dispersions of bivalent metal cations (PE/DOPC−DNA−M^{2+}). The aim was to evaluate the effect of the amide moiety on the transfection efficiency. These complexes form in a self-assembled manner, the DNA condensation being promoted by the metal cations. Synchrotron X-ray diffraction analysis was used to determine the structure of the complexes, which exhibit the lamellar symmetry of the L_α^c phase. The size and surface charge of the complexes have also been measured, and promising results of DNA transfections in vitro have been reported.

INTRODUCTION

Gene therapy is considered a promising approach[1] for the treatment of a wide range of diseases such as cancer,[2] AIDS,[3] and neurodegenerative[4] and cardiovascular[5] pathologies and is expected to be of paramount importance in the treatment of genetic disorders.[6] It consists of the possibility of a successful transfer of genetic material to targeted cells or tissues by means of appropriate delivery systems, which can be viral or synthetic. Viruses are characterized by high transfection efficiency but suffer from some serious disadvantages such as their immunogenic and potential oncogenic activity; on the contrary, synthetic vectors are neither immunogenic nor oncogenic, and their preparation is cheap and easy to perform, although low transfection efficiency in vivo represents an important restriction to their use. Despite these drawbacks, it is the opinion of many scientists that a safe and efficient human gene therapy (HGT) will depend on synthetic carriers.[7] Cationic liposomes are among the most studied synthetic vectors of DNA, although some inherent limiting aspects have not yet been solved. They include some level of cytotoxicity[8] that causes negative effects on cells such as shrinking and inhibition of the protein kinase C (PKC), a limited stability of their complexes with plasmid DNA (lipoplexes) in serum,[9] and other factors that affect the efficiency of the transfection in vivo.[10] Despite the impressive amount of work done so far on potential synthetic vectors of DNA, fully satisfying gene transfer systems have not yet been found; however, the large amount of information collected, which has allowed a thorough understanding of the relationships between physicochemical properties of the vectors and their complexes with DNA and transfection processes, is extremely important.[11] In order to increase this efficiency, the search for more stable and more efficient vectors is therefore of great importance. Neutral lipids,

Received: March 18, 2011
Revised: July 19, 2011
Published: July 26, 2011

dx.doi.org/10.1021/jp202577u | *J. Phys. Chem. B* 2011, 115, 10198–10206

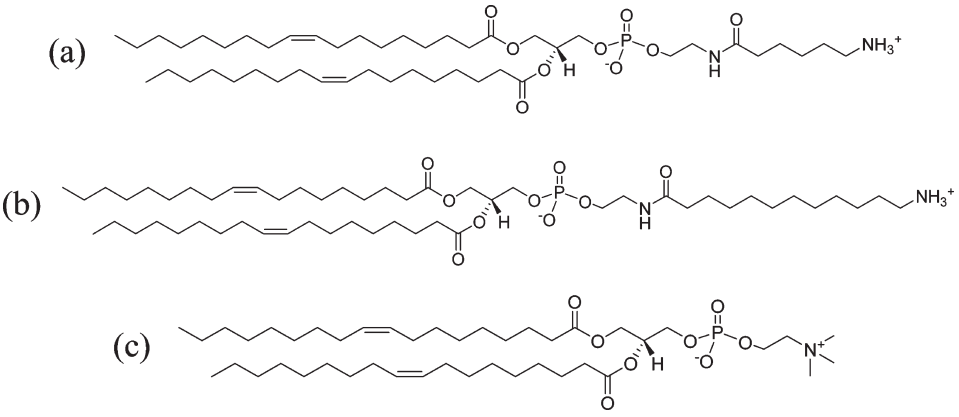

Figure 1. (a) Chemical formulas of 1,2-dioleoyl-*sn*-glycero-3-phosphoethanolamine-*N*-hexanoylamine (6PE), (b) 1,2-dioleoyl-*sn*-glycero-3-phosphoethanolamine-*N*-dodecanoylamine (12PE), and (c) 1, 2-dioleoyl-*sn*-glycero-3-phosphocholine (DOPC).

such as the zwitterionic DOPC (Figure 1c), are generally nontoxic and relatively stable in serum, which makes them potentially interesting gene transfer vectors,[12] though the low stability of their complexes with DNA prevents any self-use as vectors. However, it has been found that addition of cations[13−19] such as Ca^{2+}, Mg^{2+}, and Mn^{2+} leads to the formation of stable triple complexes NLs−DNA−M^{2+}; nevertheless, only few studies have been carried so far in the field of neutral liposomes (NLs) as vectors of genetic material, excluding some pioneering studies,[20,21] followed by a more systematic approach.[22] In recent years, we started an intense and systematic study of the structure of a series of complexes of DNA with neutral liposomes promoted by bivalent cations[23−28] as a prerequisite to test them in transfection experiments.[29] Studies on cationic amphiphiles have shown that the transfection efficiency depends not only on the polar head and the hydrophobic chain but also on the backbone of the connecting linker,[30,31] which allows us to check whether the low transfection efficiency of the neutral zwitterionic DOPC could be raised by the presence of an amidic group in the linker, as in the two commercially available 6PE (Figure 1a) and 12PE (Figure 1b). The reason for this choice comes from some recent studies that have shown a high transfection efficiency in vitro by a series of mono-, di-, and trilysinated cationic lipids[32] and even better results, both in vitro and in vivo, with cationic lipids based on a malonic acid amide backbone.[33]

EXPERIMENTAL METHODS

Materials and Sample Preparation. DOPC, 6PE, and 12PE were purchased from Avanti Polar Lipids Inc. (Alabaster, U.S.A.); DNA from calf thymus, anhydrous $MnCl_2$, and $CaCl_2$ were purchased from Sigma-Aldrich Co. (Stenheim, Germany). All chemicals were used without further purification, and the preparation of samples was performed using Milli-Q water. A DNA aqueous solution (13 mg/mL) was sonicated in order to induce fragmentation; the final length distribution, detected by gel electrophoresis, varied between 500 and 2000 bp. Mixtures of DOPC (78 mM) and 6PE or 12PE (17 mM), prepared by adding, respectively, 3, 9, 15, and 25 mol of PE to 100 mol of DOPC, were dissolved in chloroform; then, the solvent was removed under vacuum with a Speedvac apparatus. All of the lipidic films were suspended in 20 mM aqueous solutions of *N*-(2-hydroxyethyl)piperazine-*N*′-(2-ethanesulfonic acid) (HEPES buffer, pH = 7.4) obtained from Sigma-Aldrich Co. The aqueous suspensions of the corresponding complexes with DNA were prepared by mixing appropriate volumes of the various PE/DOPC lipid mixtures with solutions of metal chlorides (585 mM) and DNA (39 mM) to obtain the desired concentration in HEPES buffer. The samples were finally incubated 1 week at 4 °C.

X-ray Diffraction Experiments. XRD measurements were carried out at the high brilliance beamline ID02 of the European Synchrotron Radiation Facility (Grenoble, France). The energy of the incident beam was 12.5 keV (λ = 0.995 Å), the beam size was 100 × 100 μm^2, and the sample-to-detector distance was 1.2 m. The 2D diffraction patterns were collected by a CCD detector. We investigated the small angle q range from q_{min} = 0.1 nm^{-1} to q_{max} = 4 nm^{-1} with a resolution of 5 × 10^{-3} nm^{-1} (fwhm). The samples were held in a 1-mm-sized glass capillary. To avoid radiation damage, each sample was exposed to radiation for 3 s/frame. To calculate the electron density maps, the integrated intensities of the diffraction peaks were determined by fitting the data with series of Lorentz functions using a nonlinear baseline. The Lorentz correction was performed by multiplying each integrated intensity by sin θ, and the intensities were then calibrated by dividing by the multiplicity of the reflection.[34,35] The square root of the corrected peak was finally used to determine the modulus of the form factor F of each respective reflection. The electron density profile $\Delta\rho$ along the normal to the bilayers was calculated by Fourier sum

$$\Delta\rho = \frac{\rho(z) - \langle\rho\rangle}{[\langle\rho^2(z)\rangle - \langle\rho\rangle^2]^{1/2}} = \sum_{l=1}^{N} F_l \cos\left(2\pi l\frac{z}{d}\right)$$

where $\rho(z)$ is the electron density, $\langle\rho\rangle$ its average value, and N the highest order of fundamental reflection observed in the SAXS pattern; F_l is the form factor of the (00l) reflection, and d is the thickness of the repeating unit. The origin of the z axis was chosen in the middle of the lipid bilayer. The phase problem was solved by means of a pattern recognition approach based on the histogram of the electron density map,[36] and the results were found to be in agreement with those obtained with different approaches.[37,38]

Particle Size and *Z* Potential Measurements. Particle size analysis of the liposomes and of their complexes with DNA promoted by Ca^{2+} were performed by dynamic light scattering using a Malvern Zetasizer Nano ZS particle sizer (Malvern Instruments Inc. MA, U.S.A.) at 25 °C in a backscattering detection mode at an angle of 173°. Liposomes were prepared

at 0.1 mg/mL in 20 mM HEPES buffer at pH 7.5; the aqueous dispersions were sonicated for 7 min and filtered with a 0.45 μm cellulose acetate microfilter. To this suspension were added DNA and metal cations with a procedure similar to the one followed in preparing samples for X-rays and for the in vitro transfection experiments. All samples were equilibrated at 25 °C for 10 min before the measurements. The data reported in Table 4 are the intensity-based mean diameters, the relative polydispersion indexes (PdI) being obtained by a cumulate fit of the correlation functions. Zeta potentials were determined from the electrophoretic mobility by applying the Henry equation. For all samples, the data show a unimodal distribution and represent the average of at least four measures.

In Vitro Transfection Experiments. Transfection experiments were performed on NIH/3T3 mouse fibroblast cell lines (ATCC). Cells were maintained in Dulbecco's modified eagle medium (DMEM) with high stable L-glutamine (Euroclone, Italy) supplemented with 1% penicillin/streptomycin (p/s) and 10% fetal bovine serum (FBS, Euroclone, Italy) at 37 °C in a 5% CO_2 atmosphere. To evaluate the transfection efficiency of the complexes, pCMV-GLuc plasmid (Biolabs) was used to prepare the lipid−DNA−ion complexes. Cells were seeded in a 96 well plate (15−20.000 cells/well) and incubated until they were 70% confluent. Before performing the experiments, a $CaCl_2$ solution was added to the mixtures of lipids and DNA in a 1:0.1 mol ratio to obtain a 15 mM final concentration of Ca^{2+}. Mixtures were then incubated for 30 min at room temperature to allow complexes to form; they were then diluted with the medium (DMEM not supplemented with antibiotics and fetal serum) to a final volume of 100 μL/well. The cells treated with the complexes were incubated to allow transient transfection; after 6 h, the medium used for transfection was replaced with DMEM supplemented with 10% FBS and 1% p/s. All of the experiments were performed in quadruplicate. Luciferase expression was analyzed 48 h later through a Gaussian luciferase assay kit (Biolabs); the reading of the luminometric units was performed on a Wallac Victor 1420 multilabel counter, and the luminometric unit/well were normalized to the number of viable cells/well. Cell viability was determined through an Alamar blue viability assay (Invitrogen) that results in the linear range in these growth conditions based on control experiments.

Statistical Analysis. For transfection experiments, the data are represented as the mean ± SD, $n = 4$. Statistical analyses were performed using a nonparametric two-tail P-value test (Mann−Whitney). Results were considered significant when probability values were $p < 0{,}05$. The analysis was done using Instat software.

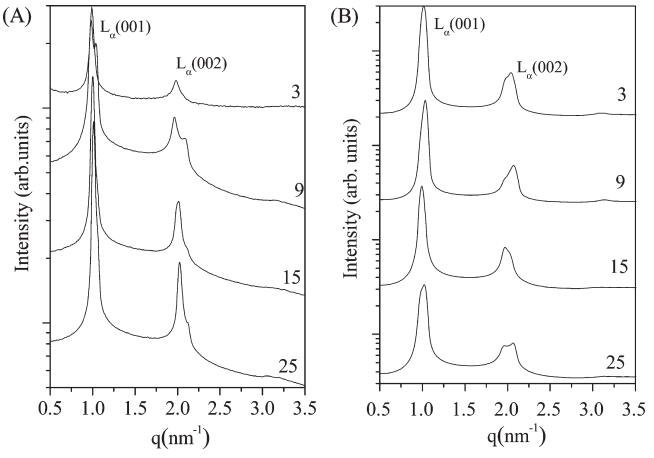

Figure 2. Small-angle XRD patterns of aqueous solutions of 6PE/DOPC (A) and 12PE/DOPC (B) mixtures at different amounts of PEs (T = 298 K). Figures reported in the patterns indicate the number of moles of PE on 100 mol of DOPC.

RESULTS AND DISCUSSION

Structure Determination by X-ray Analysis. Following a well-established procedure,[23,25,26,28] the initial step of the study has been devoted to the analysis of the structure of 6PE/DOPC and 12PE/DOPC water systems at increasing concentrations of the PE component on DOPC. The effect of the composition of the liposome mixtures on the XRD patterns is important in order to evaluate the mesomorphic behavior of the systems. Representative small-angle spectra, registered at different ratios of 6PE or 12PE with respect to DOPC at room temperature, are shown in Figure 2A and B. They consist of fairly sharp peaks centered at $q_l = 2\pi l/d$, with average d spacing values for the first order of diffraction equal to 6.3 nm for 6PE and 6.2 nm for 12PE, substantially independent from the concentration. These patterns are characteristic of a liquid-crystalline lamellar structure that corresponds to the well-known L_α phase, d spacings being

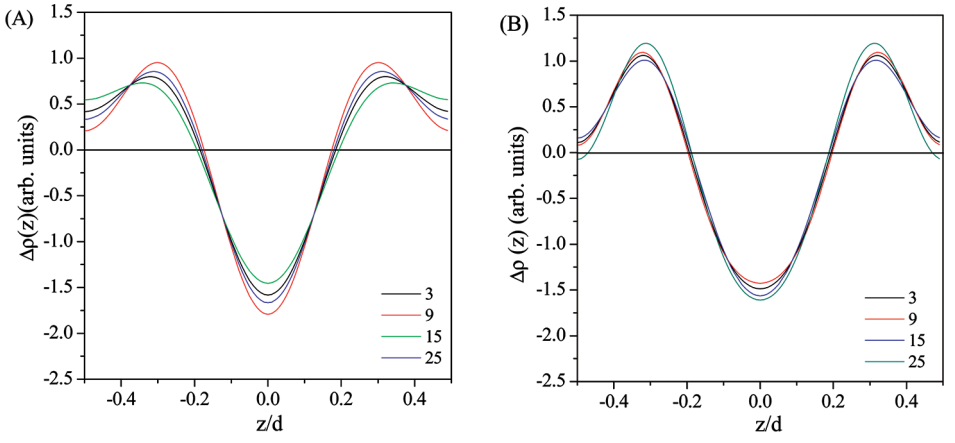

Figure 3. Electron density profiles of 6PE/DOPC (A) and 12PE/DOPC (B) as a function of the composition of the mixtures. Figures reported on the graphs indicate the number of moles of PE on 100 mol of DOPC.

Table 1. Structural Parameters Calculated for 6PE/DOPC and 12PE/DOPC

	d (nm)	d_{HH} (nm)	d_W (nm)
6PE			
3	6.4	4.0	2.4
9	6.4	3.9	2.5
15	6.3	3.8	2.4
25	6.2	3.8	2.4
12PE			
3	6.2	3.9	2.3
9	6.2	3.9	2.3
15	6.3	4.0	2.3
25	6.2	3.9	2.3
DOPC			
	6.3	3.8	2.5

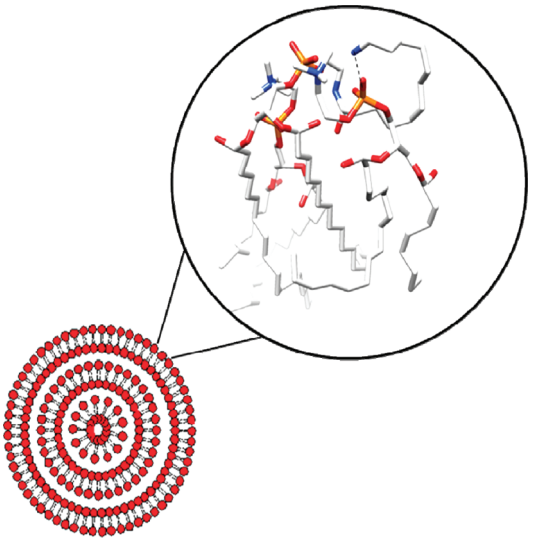

Figure 4. Amber[52] minimized structure of a monolayer portion showing two DOPC molecules interacting with a 12PE.

similar to the one of pure DOPC[37,39] (6.32 nm for fully hydrated DOPC bilayers). Some splittings are present in the peaks, a characteristic which has been found also in the X-ray spectrum of the fully hydrated DOPC.

In both mixtures of PE/DOPC as well as in pure DOPC under the same hydration conditions, the high water content between the bilayers leads to high lattice disorder, as proven by the existence of only two orders of diffraction peaks. This is normal for fully hydrated bilayers of lipids in the L_α phase, where the high bilayer fluctuation reduces the intensity of higher-order reflections[40] and makes the determination of the electron density profiles and then of the thickness of the lipid bilayers not too accurate. However, in Figure 3, the electron density profiles along the normal to the bilayers calculated as a function of PE/DOPC compositions are reported. Each large central minimum corresponds to the region of the hydrocarbon tails, and the two maxima correspond to the polar head groups; the large width of these maxima confirms a molecular disorder caused by the fluctuation of the bilayers.[41] The distance d_{HH} between the

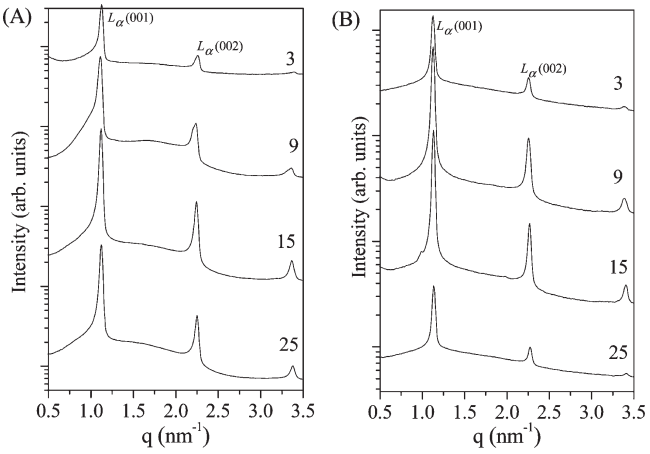

Figure 5. SAXS pattern of 6PE/DOPC−Mn^{2+} (A) and 6PE/DOPC−Ca^{2+} (B) at a molar ratio of lipids to cations of 1:3. Figures reported in the patterns indicate the number of moles of PE on 100 mol of DOPC.

two electron density maxima is generally taken as an approximation of the bilayer thickness.

Table 1 reports the data calculated for the lamellar repeat distance (d), which is the sum of the lipid bilayer thickness (d_{HH}) and the water space (d_W) between the bilayers. The average values are $d_{HH} \approx 3.9$ nm and $d_W \approx 2.4$ nm for 6PE/DOPC and $d_{HH} \approx 3.9$ nm and $d_W \approx 2.3$ nm for 12PE/DOPC. These parameters are very similar to the ones of pure DOPC, reported in the same table, and the whole of data indicates a substantial independence from the presence of increasing amounts of both 6PE and 12PE. The best fits calculated for fully hydrated DOPC at the temperature of 30 °C with different theoretical methods[40] are $d_{HH} = 3.69$ nm and $d_W = 2.72$ nm, not so far from the values determined in this work from the electron density profiles; it follows that the values obtained for the different mixtures 6PE/DOPC and 12PE/DOPC can be considered reliable, at least for the purposes of this study.

Nevertheless, these results raise some questions that need to be addressed, namely (i) how to explain the substantial identity of the data reported in Table 1 and (ii) what explanation, if there is one univocal, for the Bragg peak splittings. Referring to the first question, one may expect that the presence of the extended groups, introduced by the amidic chains, could lead to higher d values, in particular, in mixtures containing 12PE, a hypothesis that clearly conflicts with the observation that the d values for mixtures of 12PE/DOPC are substantially equal, or even lower, than the ones of pure DOPC and that the same behavior occurs for d_W. It has been argued[42] that the thickness of the water layer interposed between the bilayers in neutral liposomes is the result of a critical balance of at least four different kinds of interactions, repulsive hydration force, van der Waals attraction, which limits multilayer hydration, repulsion due to thermal undulation of the whole bilayer, and steric interaction, which has to do with the nature of the polar groups. The repulsive hydration force arises from the structuring of the water molecules at the lipid polar surface. Some authors[43,44] calculated the total number of water molecules per phospholipid in membrane bilayers and their partition between the ones intercalated in the polar head group regions and those present in the fluid space between adjacent bilayers; regardless of the numerical results of this calculations by the different authors, it was found that fully hydrated PE bilayers are separated by a number of water molecules smaller than the

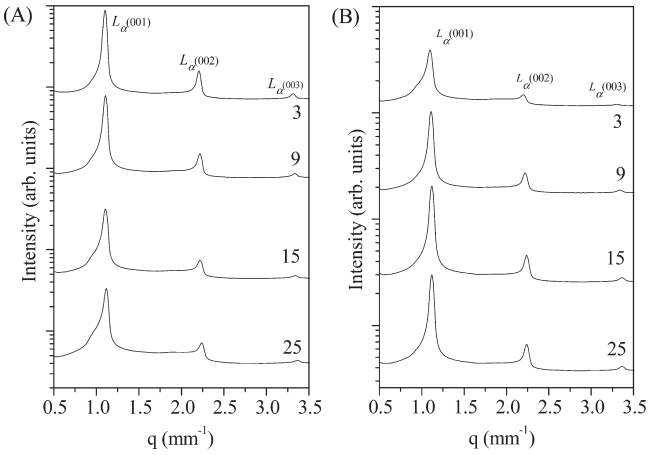

Figure 6. SAXS pattern of 12PE/DOPC−Mn^{2+} (A) and 12PE/DOPC−Ca^{2+} (B) at the molar ratio of lipids to cations of 1:3. Figures reported in the patterns indicate the number of moles of PE on 100 mol of DOPC.

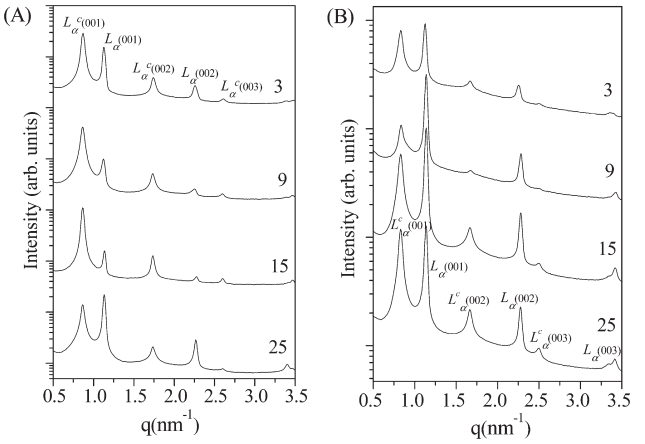

Figure 7. (A) SAXS patterns of 6PE/DOPC−DNA−Mn^{2+} and (B) 6PE/DOPC−DNA−Ca^{2+} complexes at different compositions of PE (3−25)/100 DOPC. All samples were prepared to reach a final molar ratio lipid:DNA:M^{2+} equal to 2:1:6.

Table 2. Structural Parameters Calculated for 6PE/DOPC and 12PE/DOPC in the Presence of Mn^{2+} and Ca^{2+}

	d (nm)	d_{HH} (nm)	d_W (nm)
6PE−Mn^{2+}			
3	5.6	3.9	1.7
9	5.6	3.9	1.7
15	5.6	3.8	1.8
25	5.6	3.8	1.8
12PE−Mn^{2+}			
3	5.7	3.9	1.8
9	5.7	3.8	1.8
15	5.6	3.9	1.7
25	5.6	3.9	1.7
6PE−Ca^{2+}			
3	5.6	3.7	1.9
9	5.6	3.7	1.9
15	5.5	3.7	1.8
25	5.5	3.7	1.8
12PE−Ca^{2+}			
3	5.7	4.0	1.7
9	5.7	3.9	1.8
15	5.6	3.9	1.7
25	5.6	3.9	1.7

ones of PC. van der Waals interactions are certainly affected by the polarized amidic groups, with the consequence of an increased interbilayer attraction. More troublesome is the evaluation of the remaining two parameters, which, in a rough analysis, could be interpreted as operating an expansion of the interbilayer water volume. However, in our opinion, this effect must be of limited impact and perhaps such as to substantially compensate the effect of van der Waals attraction; as a matter of fact, one can consider that a hydrophobic effect could act on the hydrocarbon part of the amidic chains, particularly on 12PE, and then force the chains themselves to assume compact arrangements, limiting any increase of the hydration pressure. Both steric interaction and thermal undulation must depend on the degree of freedom of the amidic chains, namely, in 12PE. It has been reported[45] that due to intra- and intermolecular interactions of the heads groups, phopsphatidylcholine and phosphatidylethanolamines exhibit a preferred conformation, where phosphate and ammonium nitrogen dipoles (P^- N^+) are oriented approximately parallel to the plane of the bilayers either in the gel or in the liquid-crystalline state.[46−48] Most important, this orientation does not depend on the state of hydration nor on the structure of added molecules.[49−51] Starting form these findings, it is possible to design a model in which the nonmethylated ammonium group of the PE moiety allows the formation of a strong electrostatic interaction and the formation of hydrogen bonds with the phosphate oxygen of the adjacent lipid DOPC. The consequence is that the functionalized lipids will expose their folded chain to the aqueous layer (Figure 4). This conformation can explain why the aqueous layers between 12PE/DOPC bilayers have approximately the same thickness as the one of DOPC.

As far as the second question is concerned, some literature reports can help make the situation clear. The possibility that phase separation occurs in mixtures of different lipids is documented but limited to mixtures of lipids having different hydrocarbon tails, like the saturated DPPC and the unsaturated 1,2-bis (2,4-octadecadienoyl)-3-phosphatidylcholine (DODPC).[53] All of the lipids considered in the present work refer to the same unsaturated chain; if a phase separation occurs, this should depend on hydrophobic interactions between the head group chains and not between the hydrocarbon tails. However, a recent TOF-SIMS (time of flight secondary ion mass spectroscopy) investigation of ternary lipid mixtures composed of sphingomyelin, cholesterol, and phosphatidylcholine or other PC lipids revealed that the acyl chain saturation is the dominating factor in determining phase separation.[54] It has been also reported[55] that 1:1 mixtures of lipids bearing saturated/unsaturated hydrocarbon chains, which display a single lattice in pure water, show two distinct lamellar phases when dissolved in 30 mM $CaCl_2$. In the case of the mixture DLPC/DOPC, whose hydrocarbon chains are structurally similar to the ones of the present work, d spacings are 5.83 nm in pure water against 5.96 and 7.21 nm in

Ca^{2+} solution; though we operate with a smaller amount of Ca^{2+}, no traces of peak splitting appear under these conditions. Phase separation being excluded, it seems that the splitting of the Bragg peaks should be interpreted as due to a random dispersion of the multilamellar vesicles formed in the sample preparation.

To better evaluate the formation of the ternary complexes PE/DOPC−DNA−M^{2+}, the second step of the work has been focused on the effect of bivalent metal cations (namely, Ca^{2+} and Mn^{2+}) on the polymorphic behavior of 6PE/DOPC and 12PE/DOPC. As stated by the so-called Hofmeister or lyotroipic series, bivalent cations have a "salting in" effect and, due to their high affinity for the zwitterionic head groups of lipids, easily form lipid−salt aggregates; this interaction has the effect of modifying some properties of the membrane. At a 1:3 molar ratio of lipids versus cations, new lamellar phases have been obtained and are reported in Figures 5 A, B and 6 A, B. These new lamellar phases are characterized by d values ranging from an average of 5.6 nm for 6PE/DOPC−Mn^{2+} and 6PE/DOPC−Ca^{2+} to 5.7 nm for 12PE/DOPC−Mn^{2+} and 12PE/DOPC−Ca^{2+}. As already observed,[23] hydrated cations shift the diffraction peaks toward high scattered angles, reducing the layer spacing; this reduction corresponds to an average of approximately 11% for 6PE and 8% for 12PE, the effect of Ca and Mn ions being substantially equal in both cases. The data reported in Table 2 show that the bilayers thickness d_{HH} is practically unaffected by the cations, which, on the contrary, make the interbilayer steric water thickness d_W decrease significantly, which means that metal cations induce a partial dehydration of the interbilayer water thickness, an effect that has been already reported.[23,56] As shown below, this situation characterizes also the process of formation of the quaternary complexes PE/DOPC−DNA−M^{2+} and was already found in the complex DPPC−DNA−Ca^{2+}; it was proposed[17] that also the procedure followed for the sample preparation can affect the phase behavior.

Numerous papers are dealing with the effect of cations (mainly, Ca^{2+} and Mg^{2+}) on the bilayer interactions, and the results obtained and their interpretation do not always agree. The key topic of the debate is based on the acknowledge that the equilibrium interbilayer distance is the result of a balance among the attractive van der Waals forces[57] on one side and the repulsive hydration[42] and undulation[58] ones on the other. In an early work,[59] it was found that DPPC bilayers immersed in dilute $CaCl_2$ solution separate indefinitely, but at increasing concentrations, a progressive decrease in the bilayers separation was observed. It was generally assumed that if Ca^{2+} ions have a concentration likely to be completely entrapped in the polar heads of the lipids, d_W increases due to an increased electrostatic repulsion;[55,59−61] if instead the salt concentration increases to let

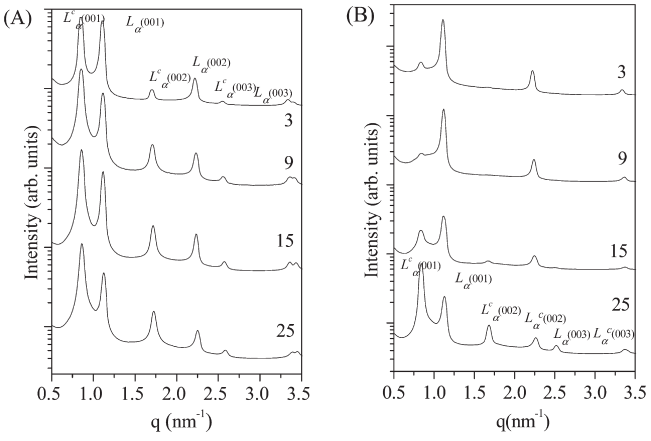

Figure 8. SAXS patterns of 12PE/DOPC−DNA−Mn^{2+} (A) and 12PE/DOPC−DNA−Ca^{2+} (B) complexes at different compositions of PE (3−25)/100 DOPC. All samples were prepared to reach a final molar ratio lipid:DNA:M^{2+} equal to 2:1:6.

Table 3. Structural Parameters Calculated for 6PE/DOPC−DNA−Mn^{2+} and 12PE/DOPC−DNA−Mn^{2+}

	d (nm)	d_{HH} (nm)	d_W (nm)
6PE			
3	7.2	4.4	2.8
9	7.3	4.5	2.8
15	7.3	4.5	2.8
25	7.3	4.3	3.0
12PE			
3	7.5	4.4	3.1
9	7.4	4.6	2.8
15	7.4	4.4	3.0
25	7.3	4.3	3.0

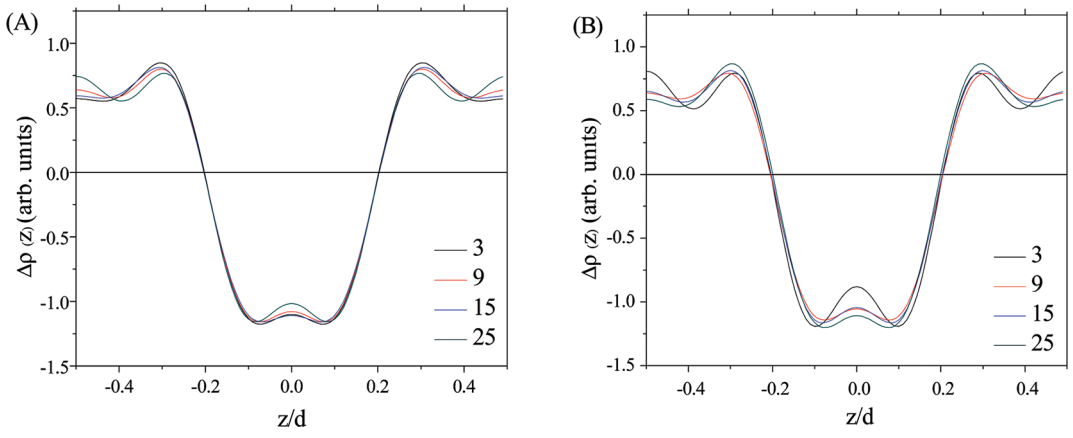

Figure 9. Electron density profiles calculated for 6PE/DOPC−DNA−Mn^{2+} (A) and 12PE/DOPC−DNA−Mn^{2+} (B) complexes as a function of the composition of mixtures.

Table 4. Sizes and Zeta Potentials of 6PE/DOPC and 12PE/DOPC Mixtures and of Their Corresponding Complexes[a]

lipid composition on 100 DOPC	size (nm)	PdI	Zeta potential (mV)
6PE(15)/DOPC	122.7(±1.8)	0.34(±0.02)	−1.7(±0.7)
6PE(25)/DOPC	102.4(±1.0)	0.26(±0.01)	−12.0(±1.1)
6PE(50)/DOPC	111.9(±1.1)	0.22(±0.01)	−14.00(±0.02)
6PE(15)/DOPC−DNA−$CaCl_2$(2/1/6)	109.6(±0.9)	0.27(±0.01)	−6.8(±0.2)
6PE(25)/DOPC−DNA−$CaCl_2$(2/1/6)	109.5(±1.8)	0.33(±0.02)	−20.6(±1.7)
6PE(50)/DOPC−DNA−$CaCl_2$(2/1/6)	175.3(±3.6)	0.25(±0.01)	−31.8(±0.5)
6PE(15)/DOPC−DNA(2/1)[a] in $CaCl_2$ 15 mM	376.5(±9.3)	0.28(±0.02)	13.6(±0.5)
6PE(25)/DOPC−DNA(2/1)[a] in $CaCl_2$ 15 mM	162.9(±2.4)	0.49(±0.02)	6.6(±0.1)
6PE(50)/DOPC−DNA(2/1)[a] in $CaCl_2$ 15 mM	139.7(±1.1)	0.21(±0.01)	5.8(±0.3)
12PE(15)/DOPC	107.3(±0.9)	0.26(±0.01)	−16.3(±2.6)
12PE(25)/DOPC	139.6(±12.2)	0.33(±0.05)	−11.3(±0.4)
12PE/DOPC(50)	93.6 (±1.0)	0.30 (±0.03)	−16.3 (±2.0)
12PE(15)/DOPC−DNA−$CaCl_2$(2/1/6)	105.2(±1.8)	0.26(±0.01)	−19.0(±3.3)
12PE(25)/DOPC−DNA−$CaCl_2$(2/1/6)	148.6(±14.2)	0.34(±0.05)	−19.6(±0.8)
12PE(50)/DOPC−DNA−$CaCl_2$(2/1/6)	93.0 (±1.5)	0.34 (±0.03)	−15.0 (±1.4)
12PE(15)/DOPC−DNA(2/1)[a] in $CaCl_2$ 15 mM	134.8(±4.9)	0.44(±0.01)	13.8(±1.0)
12PE(25)/DOPC−DNA(2/1)[a] in $CaCl_2$ 15 mM	415.0(±17.0)	0.54(±0.05)	10.6(±0.1)
12PE(50)/DOPC−DNA(2/1)[a] in $CaCl_2$ 15 mM	288.8 (±5.203)	0.61 (±0.05)	8.5 (±0.6)

[a] The compositions that show the mixtures for optimal transfections.

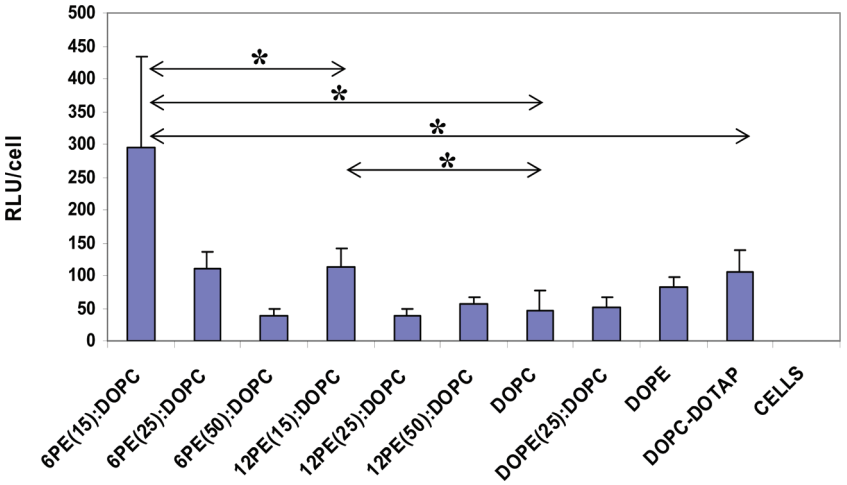

Figure 10. Luciferase expression following transfection procedure with different complexes in the NIH3T3 cell line. Expression efficiency is expressed as relative luminometric units per cell (RLU/cell) (mean + SD, $n = 4$). Statistical significance between groups is shown; $^*p < 0.05$.

hydrated ions fill the water layer between two adjacent polar heads, d_W decreases because these ions act as screening to the electrostatic repulsion.[55,59,60,62]

Finally, the structures of the two complexes PE/DOPC−DNA−M^{2+} (M = Ca and Mn) in aqueous solution have been characterized using a 2:1:6 molar ratio of lipid/DNA/M^{2+}, which has been found as the best for efficient complexation. Figure 7 refers to complexes of 6PE with Mn^{2+} (A) and Ca^{2+} (B), while Figure 8 refers to the corresponding complexes of 12PE; in all cases, the diffraction patterns exhibit clearly two distinct sets of peaks that are labeled as $L_\alpha{}^c$ and L_α. The first sets of peaks, marked as ($L_\alpha{}^c$), are due to the quaternary complexes and show higher d values, namely, 7.3 (Mn^{2+}) and 7.6 nm (Ca^{2+}) for 6PE/DOPC−DNA−M^{2+} and 7.4 (Mn^{2+}) and 7.5 nm (Ca^{2+}) for 12PE/DOPC−DNA−M^{2+}. The second set, marked as (L_α), corresponds to the self-assembled structure of the simple liposomes in the presence of metal cations (PE/DOPC−M^{2+}) and show approximately the same d value (5.5 nm for 6PE/DOPC and 5.7 nm for 12PE/DOPC) as that obtained in the absence of DNA.

As previously reported[23−28] in similar complexes, the driving force for the lipid DNA complexation must be found upon the release of the counterion entropy upon neutralization of the DNA phosphate groups by the metal cations when they form the bridge between the polar heads of the lipids and the negatively charged phosphate groups of DNA.

The formation of the quaternary complexes with DNA is confirmed by the analysis of the electron density profiles along the normal to the bilayers (Figure 9), calculated from the XRD data as a function of the composition of 6PE and 12PE. Structural

parameters of the bilayers were obtained; both profiles show an increase of the electron density in the water thickness due to the presence of the DNA confined between the lipid bilayers.

Data reported in Table 3 show that the lipid bilayers d_{HH} have a mean value of 4.4 nm for both quaternary complexes, while the mean value of the water gaps d_W is 2.8 nm for complexes with 6PE and 3.0 nm for complexes with 12PE. This water thickness is sufficient to allocate one hydrated DNA strand. The increase of the thickness of the lipid bilayers compared to those of simple lipid mixture shows a higher stiffness of the structures.

Zeta Potential and Size Determination. The characterization of the quaternary complexes PE/DOPC−DNA−M^{2+} is integrated with the determination of the particle size and the surface charge. The data reported in Table 4 assume significance in view of a possible application of these complexes as DNA vectors in gene therapy. As a matter of fact, it is known that the surface charge plays a crucial role in the process of adhesion/endocytosis that characterizes the initial step of the transfection processes with a synthetic vector of DNA. The table shows that the Z potentials of the quaternary complexes having the concentrations used on the transfection experiments (15, 25, and 50 mol of PE on 100 mol of DOPC) are all positive, as is generally requested to realize efficient transfections, and that the best efficiency is obtained in both 6PE/DOPC and 12PE/DOPC, with mixtures displaying the highest positive Z potentials. This setup allows an easy adhesion of the vector to the negative cell walls, which will promote the endocytic entrance of the system DNA vector inside of the cell. Such a correlation has not been found with the vesicle size, a parameter which is generally not strictly bound to the transfection efficiency. However, values of the size reported in Table 4 are in a range that is the one generally reported for analogous processes.

Transfection Results. The results of the transfection experiments, reported in Figure 10, show that the low efficiency of DOPC is increased by the addition of both 6PE and 12PE (with a higher effect for 6PE) and that this result occurs using the lowest molar ratios PE/DOPC (15:100), which correspond to the highest values of the Z potential. Furthermore, the 6PE(15)/DOPC complex shows a significant higher efficiency than the cationic liposome DOPC/DOTAP.

CONCLUSIONS

The data presented in this paper allow some interesting remarks. First of all, the result of the DNA transfection with 6PE(15)/DOPC−DNA−Ca^{2+}, which emphasizes an efficiency 2.7 times higher than the one of a classical cationic vector like DOPC−DOTAP, almost under the conditions of the experimental procedures followed in this work, is important because it shows for the first time that neutral lipids could be seriously considered as an alternative to cationics. If confirmed by subsequent similar results, this could be a flywheel for extensive research activity in the field of neutral liposomes as carriers of DNA, for nontoxic HGT applications. Besides, the finding that the transfection efficiency of both 6PE(15)/DOPC−DNA−Ca^{2+} and 12PE(15)/DOPC−DNA−Ca^{2+} is higher than (or similar to) the one of pure DOPE may represent an important contribution to the search for new DNA vectors of increased efficiency and safety. It is known that DOPE is characterized by a highly fusogenic inverted hexagonal phase H_{II}^{C}, a structure that is considered more favorable for improved transfection efficiencies than the lamellar one. The question about which is better between inverted the hexagonal or lamellar phase in determining the transfection efficiency is important and shows an interesting evolution in recent years. It has been found that some DNA cationic lipid complexes containing 70% DOPE instead of DOPC show a higher transfection efficiency,[63,64] but it has been also found[65,66] that some different vectors forming lamellar complexes are able to transfect with efficiencies comparable with the ones characterized by hexagonal phases. To explain the difference between low and high transfection efficiency lamellar structures, it has been proposed and documented[67] that two different paths are followed in the particular step of the entry of the vector into the cells. This result raises the question of which is the specific mechanism followed by complexes of DNA with zwitterionic lipids in the presence of cations; in this, work the effect of the cations and of their concentration on the transfection efficency has not been considered, but it cannot be escaped. Some of the data concerning the behavior of the different systems reported in this work can be used as valuable starting information for this study.

AUTHOR INFORMATION

Corresponding Author

*E-mail: m.pisani@univpm.it.

REFERENCES

(1) Patil, S. D.; Rhodes, D. G.; Burgess, D. J. *AAPS J.* **2005**, *7* (1), E61–E77.
(2) Samaranayake, H.; Määttä, A. M.; Pikkarainen, J.; Ylä-Herttuala, S. *Hum. Gene Ther.* **2010**, *21* (4), 381.
(3) Tsygankov, A. Y. *Curr. Opin. Invest. Drugs* **2009**, *10* (2), 137.
(4) Patel, S. C.; Bhupendrasinh, F. C.; Shah, K. K.; Patel, M. M. *J. Pharm. Res.* **2010**, *3* (5), 1139.
(5) Fishbein, I.; Chorny, M.; Levy, R. J. *Curr. Opin. Drug Discovery Dev.* **2010**, *13*, 203.
(6) Feng, Y.; Jacobs, F.; Van Craeyveld, E.; Lievens, J.; Snoeys, J.; Van Linthout, S.; De Geest, B. *Gene Ther.* **2010**, *17* (2), 288.
(7) Kostaleros, K.; Miller, A. D. *Chem. Soc. Rev.* **2005**, *34*, 970.
(8) Lv, H.; Zhang, S.; Wang, B.; Cui, S.; Hyan, J. *J. Controlled Release* **2006**, *114*, 100.
(9) Foradada, M.; Pujol, M. D.; Bermudez, J.; Esterlich, J. *Chem. Phys. Lipids* **2000**, *104*, 133.
(10) Dass, C. R. *J. Med. Chem.* **2004**, *82*, 579.
(11) Barteau, B.; Chèvre, R.; Letrou-Bonneval, E.; Labas, R.; Lambert, O.; Pitard, B. *Curr. Gene Ther.* **2008**, *8*, 313.
(12) Bruni, P.; Francescangeli, O.; Marini, M.; Mobbili, G.; Pisani, M.; Smorlesi, A. *Mini Rev. Org. Chem.* **2011**, *8* (1), 38.
(13) Budker, V. G.; Kazatchkov, Y. A.; Naumova, L. P. *FEBS Lett.* **1978**, *95*, 143.
(14) Kharakoz, D. P.; Khusainova, R. S.; Gorelov, A. V.; Dawson, K. A. *FEBS Lett.* **1999**, *466*, 27.
(15) Fedorov, B. B.; D'yachkov, P. N.; Zdanov, R. J. *Russ. Chem. Bull.* **1999**, *48*, 2046.
(16) Bruni, P.; Cingolani, F.; Iacussi, M.; Pierfederici, F.; Tosi, G. *J. Mol. Struct.* **2001**, *565−566*, 237.
(17) Mc Manus, J. J.; Radler, J. O.; Dawson, K. A. *J. Phys. Chem. B* **2003**, *107*, 9869.
(18) Gromelski, S.; Brezesinski, G. *Langmuir* **2006**, *22*, 6293.
(19) Tresset, G.; Cheong, W. C. D.; Tan, Y. L. S.; Boulaire, J.; Lam, Y. M. *Biophys. J.* **2007**, *93*, 637.
(20) Papahadjopoulos, D.; Vail, W. J.; Pangborn, W. A.; Poste, G. *Biochim. Biophys. Acta* **1976**, *448*, 265.
(21) Newton, C.; Pangborn, W.; Nir, S.; Papahadjopoulos, D. *Biochim. Biophys. Acta* **1978**, *506*, 281.
(22) Bailey, A. L.; Sullivan, S. M. *Biochim. Biophys. Acta* **2000**, *1468*, 239.

(23) Francescangeli, O.; Stanic, V.; Gobbi, L.; Bruni, P.; Iacussi, M.; Tosi, G.; Bernstorff, S. *Phys. Rew. E* **2003**, *67*, 11904.
(24) Francescangeli, O.; Stanic, V.; Lucchetta, D. E.; Bruni, P.; Iacussi, M.; Cingolani, F. *Mol. Cryst. Liq. Cryst.* **2003**, *398*, 259.
(25) Francescangeli, O.; Pisani, M.; Stanic, V.; Bruni, P.; Weiss, T. M. *Europhys. Lett.* **2004**, *67* (4), 669.
(26) Pisani, M.; Bruni, P.; Conti, C.; Giorgini, E.; Francescangeli, O. *Mol. Cryst. Liq. Cryst.* **2005**, *434*, 643.
(27) Pisani, M.; Fino, V.; Bruni, P.; Di Cola, E.; Francescangeli, O. *J. Phys. Chem. B* **2008**, *112* (17), 5276.
(28) Pisani, M.; Fino, V.; Bruni, P.; Francescangeli, O. *Mol. Cryst. Liq. Cryst.* **2009**, *500*, 132.
(29) Bruni, P.; Pisani, M.; Amici, A.; Marchini, C.; Montani, M.; Francescangeli, O. *Appl. Phys. Lett.* **2006**, *88*, 73901.
(30) Choi, J. S.; Lee, E. J.; Jang, H. S.; Park, J. S. *Bioconjugate Chem.* **2001**, *12*, 108.
(31) Liu, D.; Hu, J.; Qiao, W.; Li, Z.; Zhang, S.; Cheng, L. *Bioorg. Med. Chem. Lett.* **2005**, *15*, 3147.
(32) Karmali, P. P.; Kumar, V. V.; Chaudhuri, A. *J. Med. Chem.* **2004**, *47*, 2123.
(33) Heinze, M.; Brezesinski, G.; Dobner, B.; Langner, A. *Bioconjugate Chem.* **2010**, *21*, 696.
(34) Turner, D. C.; Gruner, S. M. *Biochemistry* **1992**, *31*, 1340.
(35) Harper, E.; Mannock, D. A.; Lewis, R. N. A. H.; McElhaney, R. N.; Gruner, S. M. *Biophys. J.* **2001**, *81*, 2693.
(36) Francescangeli, O.; Rinaldi, D.; Laus, M.; Galli, G.; Gallot, B. J. *J. Phys. II* **1996**, *6*, 77 and references therein.
(37) Tristram-Nagle, S.; Peytrache, H. I.; Nagle, J. F. *Biophys. J.* **1998**, *75* (2), 917.
(38) Worthington, C. R.; Khare, R. S. *Biophys. J.* **1978**, *23*, 407.
(39) Ulrich, A. S.; Sami, M.; Watts, A. *Biochim. Biophys. Acta* **1994**, *1191*, 225.
(40) Nagle, J. F.; Tristram-Nagel, S. *Biochim. Biophys. Acta* **2000**, *1469*, 159.
(41) Wiener, M. C.; White, S. H. *Biophys. J.* **1991**, *59*, 162.
(42) Rand, R. P.; Parsegian, V. A. *Biochim. Biophys. Acta* **1989**, *988*, 351.
(43) McIntosh, T. J.; Simon, S. A. *Biochemistry* **1986**, *25*, 4948.
(44) Pabst, G.; Rappolt, M.; Amenitsch, H.; Laggner, P. *Phys. Rev. E* **2000**, *62*, 4000.
(45) Hauser, H.; Pascher, I.; Pearson, R. H.; Sundell, S. *Biochim. Biophys. Acta* **1981**, *650*, 21.
(46) Sakurai, I.; Iwayanagi, S.; Sakurai, S.; Seto, T. *J. Mol. Biol.* **1977**, *117*, 285.
(47) Lesslauer, W.; Cain, J. E.; Blaise, J. K. *Proc. Natl. Acad. Sci. U.S.A.* **1972**, *69*, 1499.
(48) Zaccai, G.; Blaise, J. K.; Schoenborn, B. P. *Proc. Natl. Acad. Sci. U.S.A.* **1975**, *72*, 376–380.
(49) Franks, N. P. *J. Mol. Biol.* **1976**, *100*, 345.
(50) Worcester, D. L.; Franks, N. P. *J. Mol. Biol.* **1976**, *100*, 359.
(51) McIntosh, T. J. *Biochim. Biophys. Acta* **1978**, *513*, 43.
(52) Weiner, J. S.; Kollman, P. A.; Case, D. A.; Singh, U. C.; Ghio, C.; Alagona, G.; Profeta, S.; Weiner, P. A., Jr. *J. Am. Chem. Soc.* **1984**, *106*, 765.
(53) Tsuchida, E.; Seki, N.; Ohno, H. *Makromol. Chem.* **1986**, *187*, 1351.
(54) Zheng, L.; McQuaw, C. M.; Ewing, A. G.; Winograd, N. *J. Am. Chem. Soc.* **2007**, *129*, 15730.
(55) Lis, L. J.; Lis, W. T.; Parsegian, V. A.; Rand, R. P. *Biochemistry* **1981**, *20*, 1771.
(56) Uhríková, D.; Hanulová, M.; Funari, S. S.; Kushainova, R. S.; Šeršeň, F.; Balgavỳ, P. *Biochim. Biophys. Acta* **2005**, *1713*, 15.
(57) Ninham, B. W.; Parsegian, W. A. *J. Chem. Phys.* **1970**, *53*, 3398.
(58) Roux, D.; Safinya, C. R. A. *J. Phys. (Paris)* **1988**, *49*, 307.
(59) Inoko, Y.; Yamaguchi, T.; Furuya, F.; Mitsui, T. *Biochim. Biophys. Acta* **1975**, *413*, 24.
(60) Lis, L. J.; Parsegian, V. A.; Rand, R. P. *Biochemistry* **1981**, *20*, 1761.
(61) Marra, J.; Israelachvili, J. *Biochemistry* **1985**, *24*, 4608.
(62) Tatulian, S. A.; Gordelyi, V. I.; Sokolova, A. E.; Syrykh, A. G. *Biochim. Biophys. Acta* **1991**, *1070*, 143.
(63) Farhood, H.; Serbina, N.; Huang, L. *Biochim. Biophys. Acta* **1995**, *1235*, 289.
(64) Hui, S.; Langner, M.; Zhao, Y.; Ross, P.; Hurley, E.; Chan, K. *Biophys. J.* **1996**, *71*, 590.
(65) Ahmad, A.; Evans, H.; Ewert, K.; George, C. X.; Samuel, C. E.; Safinya, C. R. A. *J. Genet. Med.* **2005**, *7*, 739.
(66) Ewert, K.; Ahmad, A.; Evans, H. M.; Schmid, H. W.; Safinya, C. R. A. *J. Med. Chem.* **2002**, *45*, 5023.
(67) Lin, A. J.; Slack, N. L.; Ahmad, A.; George, C. X.; Samuel, C. E.; Safinya, C. R. A. *Biophys. J.* **2003**, *84*, 3307.